Toughening of polyamide 11 with carbon nanotubes for additive manufacturing

Jiaming Bai, Shangqin Yuan, Fei Shen, Baicheng Zhang, Chee Kai Chua , Kun Zhou & Jun Wei

Taylor & Francis
Taylor & Francis Group

Check for updates

Toughening of polyamide 11 with carbon nanotubes for additive manufacturing

Jiaming Bai[a], Shangqin Yuan[b], Fei Shen[b], Baicheng Zhang[a], Chee Kai Chua [iD][b], Kun Zhou[b] and Jun Wei[a]

[a]Singapore Institute of Manufacturing Technology, Singapore; [b]Singapore Centre for 3D Printing, School of Mechanical and Aerospace Engineering, Nanyang Technological University, Singapore

ABSTRACT
It has been reported that the addition of nanofillers/nanoparticles into the thermoplastic polymers could enhance the toughness of the polymer matrix. In this work, the mechanical and thermal properties of a multi-walled carbon nanotubes (CNT)/polyamide 11 nanocomposite for additive manufacturing was evaluated. Well-dispersed PA11/CNT nanocomposite powders were processed successfully by laser sintering. Compared to the pristine PA11, the fracture toughness of the PA11/CNT nanocomposite was enhanced by ∼54% by incorporating of only 0.2 wt% CNTs. With differential scanning calorimetry, X-ray diffraction and scanning electron microscope fractography analysis, the nanostructure and the toughening mechanism which lead to the toughness improvement was well identified and understood.

Introduction

Additive manufacturing (AM), or 3D printing, is an emerging technology which fabricates components directly from a computer-aided design (CAD) file in a layer-by-layer way, in contrast to conventional manufacturing techniques such as formative processes or subtractive methods (Chua and Leong 2017). All AM systems can be broadly categorised into liquid based (Yap and Yeong 2015), solid based and powder based. As one of the most developed AM technologies, powder-based AM technology is widely used to produce metal and plastic engineering end-used parts. Laser sintering (or selective laser sintering) uses laser as the heat source to fuse and melt polymeric powders together to predefined geometries from CAD. Laser sintering is very well known for its ability to manufacture parts with significantly greater complex shape, produce good end-product stability with little or no post-processing required (Hopkinson et al. 2006).

In theory, polymer materials in certain powder form can be processed by laser sintering. However due to the complex thermal process of laser sintering, current available laser-sintering materials are still very inadequate. By far Polyamide-based materials (PA11/PA12) remain as the most often selected laser-sintering polymers on the market (Chua and Leong 2017). Furthermore, the fistful of current available polymeric materials that can be processed by laser sintering cannot meet the necessities of all the majority of commercial products (Goodridge et al. 2012).

To tackle the materials limitations for laser sintering, more and more materials with wide range of properties have been developed in recent years (Athreya et al. 2011, Bai et al. 2014, 2015a). Incorporating a small amount of nanoparticles, polymeric nanocomposites have shown a significant improvement over the base polymer's mechanical, thermal and electrical properties (Rafiq et al. 2010, Lao et al. 2011, Mezghani et al. 2011, Wang et al. 2013, Yuan et al. 2016a, 2016b, Wang et al. 2017). Toughness, which demonstrates the ability of a polymer to absorb energy and resist creak under stress applied, is a crucial property in engineering polymer applications. Previous studies have shown that nanoparticles can be well dispersed in the polymer to reinforce the toughness of the matrix (Zhang and Zhang 2007, Cai and Song 2015). In the present work, carbon nanotubes (CNT), an ideal nanoparticle to reinforce polymer matrices, was incorporated with Polyamide 11 successfully to produce PA11/CNT nanocomposite powders. The PA11/CNT nanocomposite, along with pristine PA11, was laser sintered successfully to evaluate the fracture toughness. The toughening mechanism was well analysed and explained by fractography of the tested specimens.

Experiment and methods

In this work, the thermoplastic polyamide 11 (PA11) powder used as polymer matrix was obtained from EOS GmbH Germany (trade name 'PA1101').

Multiwalled CNTs, supplied by NanoAmor Materials Inc. US, had an average diameter of 20–30 nm and length of 10–30 μm. PA11/CNT nanocomposites were fabricated by a phase separation latex method, by coating the CNTs (0.2 wt%) on the surface of the PA11 particles (Figure 1) (Bai *et al.* 2014, Yuan *et al.* 2016a). The CNTs-coated PA11 powders were filtrated and dried after they precipitated out from the solvent. Afterwards, the residual solvent left in the nanocomposite matrix was then evaporated through further drying in an oven at 70°C for 8 h.

A commercial laser-sintering machine EOS P395 (EOS GmbH, Germany) was used to laser sinter the PA11 and PA11/CNT nanocomposite. The laser-sintering machine has a continuous CO_2 laser with a wavelength of 10.6 μm, which can generate laser power up to 50 W. In terms of ease of processing and achieving the enhanced mechanical properties, processing parameters, including powder bed temperature and laser power were optimised, shown in Table 1. The ability to absorb energy during plastic deformation reflects the toughness of a material. Impact testing is applied in this work to study the toughness of the laser-sintered PA11 and PA11–CNT. Impact test specimens ($63 \times 12 \times 6$ mm^3) of both PA11 and PA11/CNT were built to establish the impact strength according to ASTM D256 (Figure 2 (c), (d)). There were eight specimens for each material tested by the Izod testing method according to ASTM D256.

Differential scanning calorimetry (DSC) was carried out using a Q200 DSC from TA Instruments under an air atmosphere at 10°C/min heating/cooling rate. The PA11 and PA11CNT powders with mass of 5 mg were encapsulated in a TA Tzero standard aluminium pan and loaded into DSC. Wide-angle X-ray diffraction (WXRD) was performed with a Rigaku (Japan) S-3000N Multiplex X-ray diffractometer at 40 kV and 20 mA with a Ni-filtered Cu Ka radiation ($k = 1.542$ Å), and scanned at a rate of 0.08°/min. A JEOL JSM-7600F, field-emission scanning electron microscope (JEOL Ltd., Tokyo, Japan) at 2–5 kV was used to characterise the surface morphologies of polymeric powders and observe the dispersion of the CNT, and the fractography of the PA11 and PA11–CNT nanocomposite.

Results and discussion

The scanning electron microscope (SEM) micrographs for the PA11 and PA11/CNT nanocomposite powders are shown in Figure 2 (a), (b). No obvious difference in the powder surface morphology between the neat and the nanocomposite powders could be seen. With high magnification, it also can be seen that the CNTs were coated and dispersed well on the surface of PA11 powder without agglomeration. This is very important for

Table 1. Processing parameters for the laser sintering of PA11 and PA11–CNT.

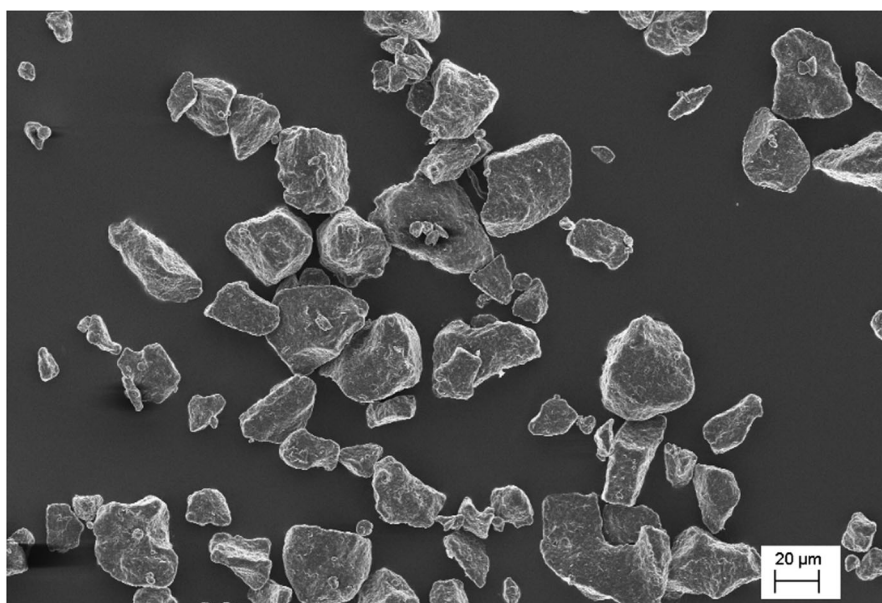| Parameters	
Powder bed temperature (°C)	181
Layer thickness (μm)	100
Laser power (W)	30
Laser scanning speed (mm/s)	3000
Laser scanning space (mm)	0.30

Figure 1. Scanning electron microscopy of the PA11–CNT nanocomposite powders.
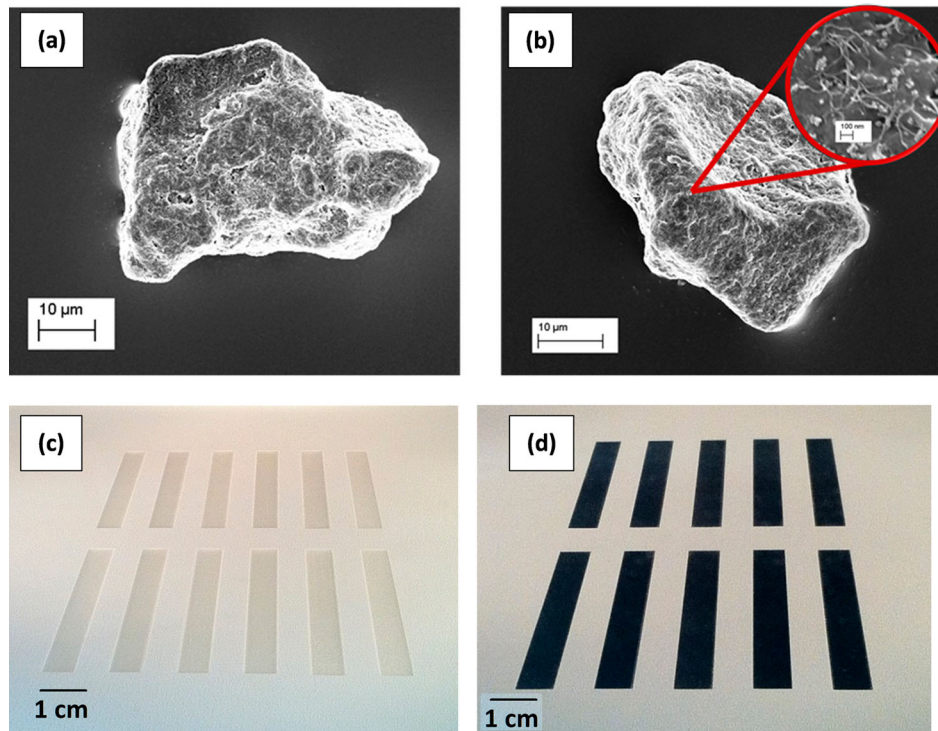
Figure 2. SEM images of (a) PA11 and (b) PA11–CNT powder particles; fabrication of impact specimens of (c) PA11 and (d) PA11–CNT by laser sintering.

nanoparticle reinforced polymer nanocomposites, as the dispersion and distribution of nanofillers in the polymer matrix are one of the most important factors affecting the properties of the nanocomposites (Bai *et al.* 2015b). Particulate nanofillers tend to form agglomerates very easily, which can weaken the properties of the final nanocomposite parts. Therefore, the nanofillers should be well dispersed in the polymer matrix to achieve optimal reinforcement effects.

Both the PA11 and PA11–CNT nanocomposite powders were easy to spread over the build area of the laser-sintering machine. The impact specimens were laser sintered successfully without any distortion. The impact strength of PA11 and PA11–CNT nanocomposites parts is recorded in Table 2. Compared to PA11, which had impact strength of 6.16 kJ/m^2, the impact strength of the PA11/CNT increased by ∼54% to 9.48 kJ/m^2. This demonstrated the strong toughness enhancement introduced by the CNT nanofillers.

The DSC tests were carried out to examine the thermal properties of the PA11 and PA11–CNT laser-

sintering parts (Figure 3 and Table 2). It can be seen that by adding CNTs into PA11, the crystallisation temperature was increased by about 5°C. This phenomenon suggests that the CNTs acted as a nucleating agent and had a nucleation effect to facilitate the crystallisation of PA11 in the cooling stage, similar to that observed by other studies (Zhang and Zhang 2007, Bai *et al.* 2013, Yuan *et al.* 2016b). However, the CNT did not alter the melting point of PA11 matrix. Crystallinity is one of the aspects to influence the final mechanical properties of semi-crystalline thermoplastic materials, as higher crystallinity normally leads to greater mechanical properties. The crystallininty is calculated as $C\% = \Delta H/\Delta H_{100\%}$, where ΔH stands as the enthalpy of melting from the DSC results, $\Delta H_{100\%}$ being enthalpy of melting for fully crystalline polymer (For PA11, the enthalpy of melting with fully crystallinity is 189 J/g Zhang *et al.* 2000). The higher crystallinity for PA11–CNT matched the impact strength enhancement in this work. The crystal sizes (τ) of the PA11 and PA11–CNT laser-sintered parts were evaluated from

Table 2. Thermal, crystal and impact properties of PA11 and PA11/CNT nanocomposite.

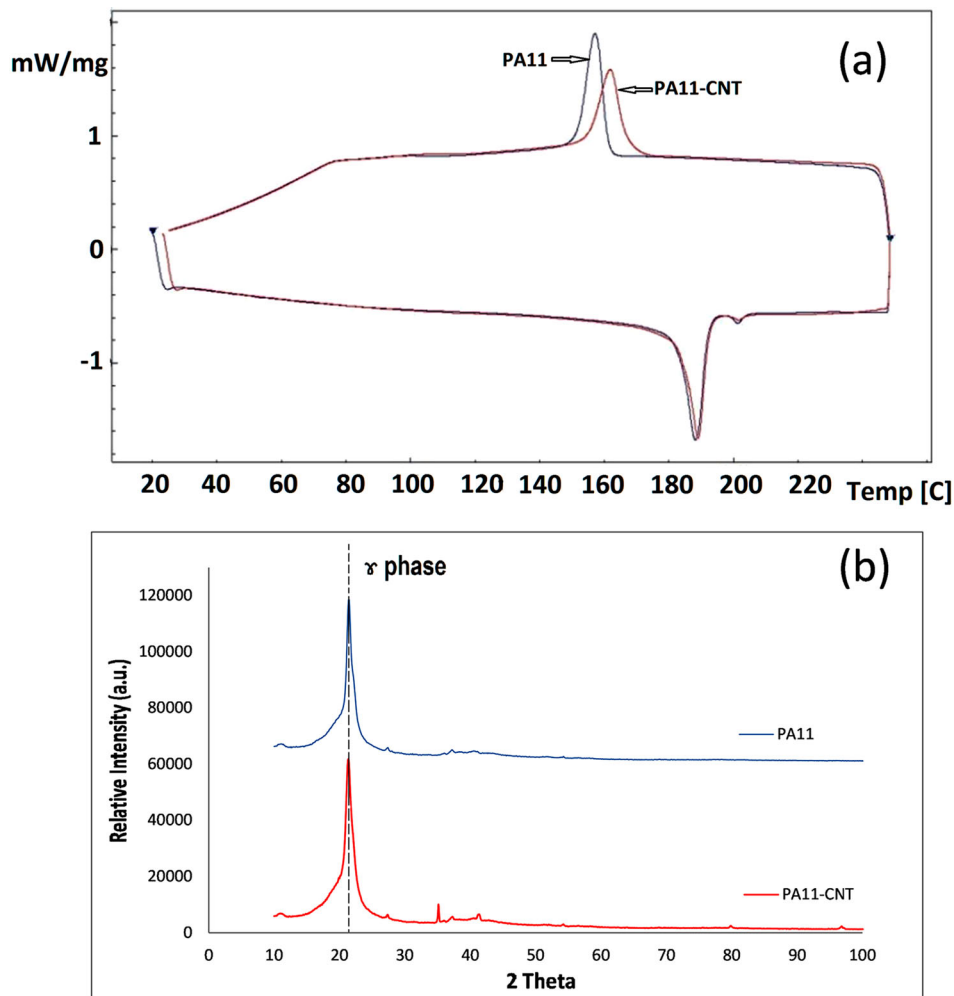|	Melting temperature (°C)	Crystallisation temperature (°C)	Crystallinity (%)	Crystal size (nm)	Impact strength (kJ/m^2)
PA11	188.2	157.3	63.1	7.41	6.16 (±0.41)
PA11–CNT	189.1	161.8	64.2	6.31	9.48 (±0.32)

Figure 3. (a) DSC curve of PA11 (blue) and PA11–CNT (red) laser-sintered parts; (b) wide-angle XRD patterns of PA11 and PA11–CNT nanocomposite.

the X-ray diffraction (XRD) results (Figure 3(b)) by the Scherrer Formula:

$$\tau = \frac{K\lambda}{B \cos(\theta)},$$

where τ is the grain size, K is the dimensionless shape factor (0.9), B is the full width at half maximum (FWHM), θ is the Bragg angle. Compared to PA11 (7.41 nm), the crystal size of the PA11–CNT decreased to 6.31 nm. Because of the much more nucleating site, the crystal size should be smaller in a limited space than that of the neat PA11, and this could also contribute the toughening of the nanocomposite. Similar phenomenon was reported for CNT toughed nanocomposite (Zhang and Zhang 2007).

The fracture surface of the laser-sintered PA11 and PA11–CNT specimens were examined by SEM. As shown in Figure 4(a), the PA11 parts had typical large oriented and allied strip patterns which generated from the impact cracks. Inside the allied strip patterns was

very smooth region, which indicate the brittleness of the fracture surface where the crack propagated rapidly (Zaman et al. 2011). These fractography observations agree well with the low toughness value of the PA11 material. Compared to PA11, the fracture surface of PA11–CNT was more homogeneous, where the large strip patterns disappeared, shown in Figure 4(b). The surface had more ditches and smaller crazes, which indicated that the cracks were deflected and distorted when propagating inside the PA11–CNT nanocomposites. It is believed that the crack will be deflected when it encounters the nanoparticles, and this induces the increment of the fracture surface area which is related to the increase in energy absorption.

When fibre is embedded in polymer, the toughness of the polymer matrix can be enhanced through energy-consuming phenomenon: crack bridging, fibre pull-out or fibre break (Johnsen et al. 2007). Crack bridging happens when a growing crack is hindered by the nano-fibres. To propagate, the crack will grow around the
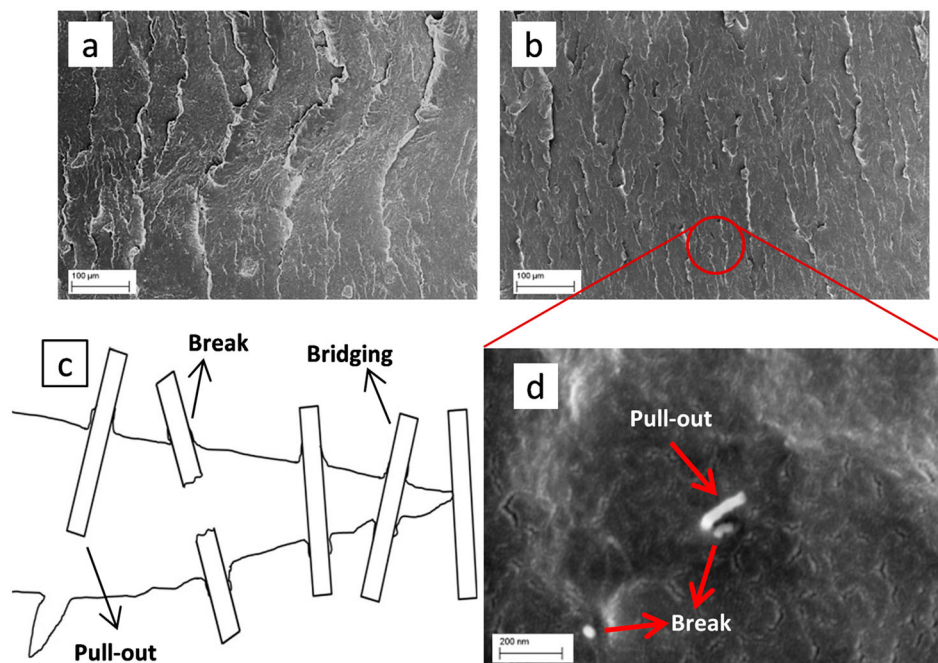
Figure 4. SEM fractography of (a) PA11 and (b) PA11–CNT laser-sintered parts; (c) schematic illustration of CNT toughness mechanism; (d) high magnification SEM fractography of PA11–CNT nanocomposite.

nanofibres rather than go through it. As the crack bridging proceeds, the fibre pull-out occurs when the fractures cover the fibre completely and the fibre comes out from the polymer matrix. If the fibre is long enough, the stress could be converted completely which will lead the breakage of the fibres (Figure 4(c)). In the current work, both fibre pull-out and fibre break happened during the impact testing for PA11–CNT nanocomposite, as shown in Figure 4(d). The breakage and pull-out of the nanotubes absorb additional energy by hindering crack propagation, which toughen the polymer matrix. Furthermore, nano size micro-cracks were also observed in the PA11–CNT nanocomposite, which also increase the total fracture surface area hence enhancing the toughness of the nanocomposite.

Conclusion

In the current work, a small amount of CNT nanofiller was incorporated into the polymer matrix, which was then processed by laser sintering successfully. Results showed that the toughness of the laser-sintered PA11 nanocomposite was improved significantly. Based on the observation and experimental investigation, the toughening effect was contributed by the deflection and distortion of the cracks when propagating inside the nanocomposites matrix, and the crack-bridging, CNT pull-out and CNT break which also absorb additional

energy by hindering crack propagation. In addition, the increased crystallinity and smaller crystal size induced by the CNT would also benefit the toughness to some extent.

Disclosure statement

No potential conflict of interest was reported by the authors.

Funding

ORCID

Chee Kai Chua http://orcid.org/0000-0001-5703-2490

References

Athreya, S.R., Kalaitzidou, K., and Das, S., 2011. Mechanical and microstructural properties of Nylon-12/carbon black composites: selective laser sintering versus melt compounding and injection molding. *Composites Sciene and Technology*, 71, 506–510.

Bai, J., et al., 2013. Improving the mechanical properties of laser-sintered polyamide 12 through incorporation of carbon nanotubes. *Polymer Engineering & Science*, 53, 1937–1946.

Bai, J., et al., 2014. Nanostructural characterization of carbon nanotubes in laser-sintered polyamide 12 by 3D-TEM. *Journal of Materials Research*, 29, 1817–1823.

Bai, J., *et al.*, 2015a. Processing and characterization of a polylactic acid/nanoclay composite for laser sintering. *Polymer Composites*. doi:10.1002/pc.23848

Bai, J., *et al.*, 2015b. Thermal influence of CNT on the polyamide 12 nanocomposite for selective laser sintering. *Molecules*, 20, 19041–19050.

Cai, D. and Song, M., 2015. Ultra-high enhancement in the toughness of polyethylene by exfoliated natural clay nanosheets. *Journal of Applied Polymer Science*, 132, n/a-n/a.

Chua, C.K., and Leong, K.F., 2017. *3D printing and additive manufacturing: principles and applications*. 5th ed. Singapore: World Scientific Publishing Company Pte Limited.

Goodridge, R.D., Tuck, C.J., and Hague, R.J.M., 2012. Laser sintering of polyamides and other polymers. *Progress in Materials Science*, 57, 229–267.

Hopkinson, N., Hague, R.J.M., and Dickens, P.M., 2006. *Rapid manufacturing: an industrial revolution for the digital age.* Chichester: John Wiley.

Johnsen, B.B., *et al.*, 2007. Toughening mechanisms of nanoparticle-modified epoxy polymers. *Polymer*, 48, 530–541.

Lao, S.C., *et al.*, 2011. Flame-retardant polyamide 11 nanocomposites: further thermal and flammability studies. *Journal of Fire Sciences*, 29, 479–498.

Mezghani, K., *et al.*, 2011. Influence of carbon nanotube (CNT) on the mechanical properties of LLDPE/CNT nanocomposite fibers. *Materials Letters*, 65, 3633–3635.

Rafiq, R., *et al.*, 2010. Increasing the toughness of nylon 12 by the incorporation of functionalized graphene. *Carbon*, 48, 4309–4314.

Wang, X., Jin, J., and Song, M., 2013. An investigation of the mechanism of graphene toughening epoxy. *Carbon*, 65, 324–333.

Wang, X., *et al.*, 2017. 3D printing of polymer matrix composites: a review and prospective. *Composites Part B: Engineering*, 110, 442–458.

Yap, Y.L., and Yeong, W.Y., 2015. Shape recovery effect of 3D printed polymeric honeycomb, *Virtual and Physical Prototyping*, 10, 91–99.

Yuan, S., *et al.*, 2016a. Highly enhanced thermal conductivity of thermoplastic nanocomposites with a low mass fraction of MWCNTs by a facilitated latex approach. *Composites Part A: Applied Science and Manufacturing*, 90, 699–710.

Yuan, S., *et al.*, 2016b. Material evaluation and process optimization of CNT-coated polymer powders for selective laser sintering. *Polymers*, 8 (10), 370.

Zaman, I., *et al.*, 2011. Epoxy/graphene platelets nanocomposites with two levels of interface strength. *Polymer*, 52, 1603–1611.

Zhang, H., and Zhang, Z., 2007. Impact behaviour of polypropylene filled with multi-walled carbon nanotubes. *European Polymer Journal*, 43, 3197–3207.

Zhang, Q., *et al.*, 2000. Influence of annealing on structure of Nylon 11. *Macromolecules*, 33, 5999–6005.